Published in final edited form as:
J Phys Chem Lett. 2010 September 2; 1(17): 2524–2529. doi:10.1021/jz100817z.

DNA Encapsulation of Ten Silver Atoms Produces a Bright, Modulatable, Near Infrared-Emitting Cluster

Jeffrey T. Petty[1,*], **Chaoyang Fan**[2], **Sandra P. Story**[1], **Bidisha Sengupta**[1], **Ashlee St. John Iyer**[2], **Zachary Prudowsky**[1], and **Robert M. Dickson**[2,*]

[1] Department of Chemistry, Furman University, Greenville, SC 29613

[2] School of Chemistry and Biochemistry and Petit Institute for Bioengineering and Bioscience, Georgia Institute of Technology, Atlanta, GA 30332

Abstract

Photostability, inherent fluorescence brightness, and optical modulation of fluorescence are key attributes distinguishing silver nanoclusters as fluorophores. DNA plays a central role both by protecting the clusters in aqueous environments and by directing their formation. Herein, we characterize a new near infrared-emitting cluster with excitation and emission maxima at 750 and 810 nm, respectively that is stabilized within $C_3AC_3AC_3TC_3A$. Following chromatographic resolution of the near infrared species, a stoichiometry of 10 Ag/oligonucleotide was determined. Combined with excellent photostability, the cluster's 30% fluorescence quantum yield and 180,000 $M^{-1}cm^{-1}$ extinction coefficient give it a fluorescence brightness that significantly improves on that of the organic dye Cy7. Fluorescence correlation analysis shows an optically accessible dark state that can be directly depopulated with longer wavelength co-illumination. The coupled increase in total fluorescence demonstrates that enhanced sensitivity can be realized through Synchronously Amplified Fluorescence Image Recovery (SAFIRe), which further differentiates this new fluorophore.

Keywords

near infrared fluorescence; few-atom silver clusters; DNA templates; Ag nanodot; optical modulation

Improved fluorescence sensitivity, largely through background reduction, continues to motivate the development of fluorescence contrast agents in the near infrared spectral region.[1] From 700–1000 nm, not only is scattering diminished relative to shorter wavelengths, but light absorption by hemoglobin, lipids, and water is also minimized.[2–3] Furthermore, endogenous chromophores typically have electronic transitions in the ultraviolet and visible spectral regions, so background autofluorescence is also drastically reduced using near infrared excitation.[1] These spectroscopic features in conjunction with cost-effective instrumentation suggest the great promise of near-infrared based molecular diagnostics.[4] However, the true potential of near infrared contrast agents is restricted by fluorophores with low sustained emission rates at low excitation (brightness), small numbers of emitted photons (photostability), and/or limited compatibility with biological environments.[5]

jeff.petty@furman.edu and dickson@chemistry.gatech.edu.

Supporting Information Available: Detailed experimental procedures and supplemental figures. This material is available free of charge via the Internet at http://pubs.acs.org.

Due to their small size (~1 kDa), organic, transition metal, and lanthanide fluorophores both minimize perturbation of biomolecular interactions and enable high labeling densities to increase detection sensitivity.[6] Also contributing to their prevalence is amenability to synthetic modifications, thereby permitting covalent attachment to specific biomolecules, enhanced aqueous solubility, and modified spectral properties.[5,7–9] Genetically expressed fluorescent proteins are also attractive fluorophores that enable direct and specific correlations of fluorescence changes with protein activity.[10] While a wide array of emitters spanning the visible spectrum have been created, extension to ~700 nm has only recently been achieved by using bacteriophytochromes.[11,12] However, like traditional organic dyes, low fluorescence quantum yields currently limit the utility of near infrared-emitting proteins. Alternatively, despite increased size and potential toxicity concerns, semiconductor quantum dots are also promising emitters for biological imaging due to their large fluorescence quantum yields, high molar absorptivities, superior photostabilities, and narrow emission spectra.[13–15] Quantum dot core composition and size influence the bandgap, and near infrared emitters have been formed using CdTe, InAs and PbSe cores.[16–18] The shell enhances photoluminescence and modification of its surface allows aqueous solubility and bioconjugation. With a hydrodynamic diameter ranging from 10–40 nm, however, these chromophores are most amenable to cell-surface labeling or analytical applications, as restricted membrane transport, toxicity, and aggregation can limit intracellular or in vivo applications.

Silver clusters are an emerging class of fluorescence contrast agents with distinct advantages.[19–22] These few-atom clusters are formed in aqueous environments using DNA templates, and their sparse energy level structure favors radiative relaxation, as indicated by fluorescence quantum yields in the 10–60% range. Molar absorptivities in the 100,000 – 400,000 $M^{-1}cm^{-1}$ range in conjunction with high photostability and unobtrusive blinking make silver clusters promising fluorescence contrast agents.[20,23] Photoinduced transitions to dark electronic states occur on short μs time scales, and near infrared absorption from these states has been used to optically control the fluorescence intensity in the visible region.[24] Central to cluster stability in aqueous environments is coordination by nucleobases of DNA. Importantly, the type of cluster, and hence its emission spectrum, is tunable by slight variations in the base sequence. Through tuning the encapsulating ssDNA sequence, we herein report on a near infrared emitting species whose brightness, photostability, spectrum, and optically controllable photodynamics establish its promise as a contrast agent for highly sensitive fluorescence imaging.

Chemical and Physical Properties

Building on our earlier studies showing that both cytosine and adenine strongly interact with silver clusters and that repeated DNA sequences provide excellent templates for fluorescent clusters in the visible region, the sequence $C_3AC_3AC_3AC_3A$ was used as an initial template for a near infrared emitting cluster.[20,25] Although the emitter can be created using this template, substitution of T for A in the 12^{th} position to give $(C_3A)_2C_3TC_3A$ dramatically improved fluorescence spectral purity, stability, and concentration. The cluster that forms with this oligonucleotide was uniquely characterized by its strong, stable emission at 810nm (λ_{ex} = 750 nm) (Fig. 1). Similar maxima in the absorbance and fluorescence excitation spectra indicate that both spectroscopic methods are probing the same electronic transition. Furthermore, circular dichroism associated with this electronic transition supports cluster association with its chiral DNA template. Diffusion times derived from fluorescence correlation spectroscopy provide the size of this DNA-bound cluster (Fig. 2). Two distinct processes contribute to the fluctuations in fluorescence intensity, and the slowest of these is attributed to passage of this fluorescent species through the confocally-defined probe

volume. As the molecular size controls transit time, a size standard provided by the organic chromophore Cy7 enables the cluster's hydrodynamic radius to be evaluated:

$$\frac{\tau_{Ag-DNA}}{\tau_{Cy7}} = \frac{r_{Ag-DNA}}{r_{Cy7}}$$

in which the τ's indicate the crossing times and the *r's* indicate the hydrodynamic radius of an equivalent sphere, with the subscripts designating the cluster-DNA conjugate or Cy7. The cluster is associated with the DNA scaffold, as evident from its longer transit time relative to that of Cy7. More quantitatively, the derived hydrodynamic radius of 2.4 ± 0.3 nm is in the size range of related DNA-cluster conugates.[20]

Although often spectrally pure in fluorescence, multiple absorption bands are common features of this and related cluster-DNA complexes. Spectral evolution with time and associated isosbestic points suggest that different types of clusters develop during the synthesis. Chemical identification of these species remains a challenge, with only correlative methods available to suggest the identity of low population, impure species.[19,26] Reversed-phase high-performance liquid chromatography of these silver clusters, however, enabled purification and further characterization of the cluster-DNA conjugates of interest (Fig. 3). Using triethylamine cations as an ion pairing agent, cluster-laden oligonucleotides were separated based on their interaction with the alkylated stationary phase.[27] Three major peaks are observed through monitoring the absorbance at 260 nm, where DNA is the dominant contributor to the spectral response. Peak III is attributed to oligonucleotides devoid of silver, as its retention time and absorption spectrum are similar to those of the oligonucleotide alone. The other two major peaks have spectroscopic signatures that indicate silver-laden oligonucleotides. Peak I has an absorption maximum of 400 nm, where prominent absorption also occurs in the crude sample (Fig. 1S). This peak is ubiquitous in all as-synthesized silver cluster samples. Upon separation, Peak II is essentially devoid of this feature, to reveal an absorption spectrum that is dominated by absorption bands associated with the nucleobases in the ultraviolet region and the silver cluster in the near infrared (Figs. 3 and 1S). This simplified spectrum highlights the relatively sparse electronic energy level structure of small silver clusters in the visible and near infrared spectral regions.[28] Further scrutiny of this particular species is provided by its unique near-infrared emission. This chromatographically resolved species was chemically characterized by separating it from the effluent and by analysis via inductively coupled plasma-atomic emission spectroscopy. With the ability to resolve the near infrared emitting species from the mixture of species, elemental analysis was used to determine the silver and phosphorus content and thus the relative silver:oligonucleotide stoichiometry of the conjugate. To account for detection efficiency of the two elements, control samples containing oligonucleotide and Ag^+ were prepared and analyzed in an identical manner as the cluster samples. For the near-infrared emitting cluster, the relative Ag:oligonucleotide stoichiometry is 9.6 ± 0.8, strongly suggesting that the empirical Ag:DNA ratio is 10:1. Further insight into the stoichiometry of the cluster and DNA strand is provided by a comparison of the absorption bands in the ultraviolet and near infrared, after purification. The prominent absorption band at 260 nm has an absorption maximum that is similar to that of DNA alone, which suggests that nucleobase absorption is most significant in this spectral region. Based on extinction coefficients of 130,000 M^{-1} cm^{-1} and 180,000 M^{-1} cm^{-1} (vida infra) for the oligonucleotide and cluster, respectively, the similar absorbances for these two electronic bands suggest a 1:1 stoichiometry of the 10-atom cluster and oligonucleotide. Given the small size of the DNA strand, it is expected that the bound silvers are strongly electronically coupled due to their proximity, and thus likely behave as a single cluster. The

spectrum of this species is distinct from those of other DNA-bound clusters and further supports a fundamental fluorescent unit comprised of 10 Ag atoms.

Photophysical Properties

The fluorescence quantum yield, molar extinction coefficient, and fluorescence lifetime underscore the distinctive photophysical properties of this particular chromophore relative to other near-infrared emitting species. Using Cy7 as a reference, the fluorescence quantum yield of the cluster is 30 ± 2%. This value is consistent with other emissive cluster-DNA conjugates, and its magnitude indicates relatively efficient radiative relaxation, in contrast to relaxation in larger nanoparticles.[29] By comparison, typically used fluorophores such as Cy7 often have low quantum yields (0.13), although significant progress has been made in developing brighter organic chromophores.[30] The Ag_{10} extinction coefficient was derived using the cluster-specific absorbance and the concentration measured by fluorescence correlation spectroscopy. Powerful features of FCS are the ability to spectrally resolve species in a complex mixture and to directly quantify their occupancy of the probe volume.[31] Using the amplitudes of the diffusive component of the correlation functions, the average number of clusters in the probe volume was determined. The interrogated volume was measured using Cy7 solutions with known concentrations, so that the average concentration of near-infrared emissive clusters in the bulk solution was determined. In conjunction with the absorbance attributed solely to the near-infrared emitting species, the extinction coefficient was determined to be 180,000 (± 50,000) M^{-1} cm^{-1}. The molecular brightness derived from the product of the fluorescence quantum yield and the molar extinction coefficient demonstrates the distinctiveness of this fluorophore with respect to its detectability. Relative to other chromophores in this spectral region, its brightness of 60,000 M^{-1} cm^{-1} is comparable to or exceeds those of spectrally similar organic chromophores.[30,32] The cluster is also predisposed to sensitive detection using high intensity laser excitation, as indicated by its fluorescence lifetime 1.8 ns (Fig. 3S) and increased relative brightness compared to dyes having longer-lived dark states that limit sustainable emission rates (see below, Fig. 2S).

Photostability provides another metric to gauge the suitability of this fluorophore for imaging applications. For these studies, the cyanine dye Cy7 and the near infrared-emitting clusters were separately dispersed and immobilized in polyvinyl alcohol to isolate single molecules (Fig. 2S). Under conditions of moderate mercury lamp excitation (~20W/cm^2), the silver clusters distinguish themselves in two ways. First, the clusters are twice as bright as the organic reference dye, which is consistent with relative brightness derived from their extinction coefficients and fluorescence quantum yields. Second, the clusters exhibit much greater photostability than does Cy7. While Cy7 exhibits single exponential decay kinetics, the clusters exhibit biexponential behavior. Based on the amplitudes from the fits, the less stable species represent 33% of the total population of clusters and have a decay rate that is 1.4 times slower than that of Cy7, yielding about 2.8 times as many total photons. The major, longer-lived fraction, however, has a decay rate that is 36 times longer than Cy7, giving ~70-fold more photons/molecule before photobleaching. The nature of this biexponential decay could be due to effects of the polyvinylalcohol matrix on the DNA. To further investigate the relative photostabilities, the two species were also evaluated in solution. Under identical conditions of 2mW laser irradiation at 690nm in a cuvette over a 2 hour time period, cluster fluorescence exhibited no discernable intensity or spectroscopic changes while Cy7 exhibited a 50% dimunition in intensity.

Further insight into the electronic structure and dynamics of the near infrared-emitting cluster is derived from the short time scale process in the fluorescence correlation functions (Fig. 2). Using a three-level system, the observed correlation times were resolved into

entrance times to (τ_{on}) and exit times from (τ_{off}) from this dark state (Fig. 2 and Table 1).[33] The effect of laser irradiance provides insight into the coupling of these higher electronic states. A decrease in τ_{on} with increasing irradiance follows from the increased population of the excited emissive state, which in turn drives occupancy of the dark state. More importantly, τ_{off} likewise decreases, which is at odds with a three-level model in which natural decay is the sole means of relaxation from the dark state to the ground electronic state. An explanation for the shortening τ_{off} is that photon absorption provides an alternative pathway for depopulating the excited dark state. For organic chromophores, nonemissive states typically have triplet multiplicity, and absorption from these states contributes to the overall photochemical kinetics when high irradiances needed for single and few molecule detection are used.[34–35] For silver clusters, the dark states have been ascribed to arise from a charge transfer state that is weakly coupled to the emissive manifold of electronic states, and they are distinguished by their large action cross section that enables efficient depopulation using low laser irradiances.[36]

The ability to exert laser control of the dark state occupancy offers the opportunity to enhance the detectability[24] of the near-infrared emitting cluster. For these experiments, a 690 nm laser induced fluorescence within the emissive manifold, while a 905 nm laser sequentially promoted excitation from the dark state. If coupling of this higher lying state with the fluorescent manifold is sufficiently strong, then reverse crossing followed by rapid relaxation to the ground electronic state will enhance the overall population in the fluorescent manifold and hence increase the fluorescence intensity (Fig. 2).[34,37] The choice of wavelengths was based on two considerations. First, minimal fluorescence background is expected from the longer wavelength excitation, and spectral filtering isolates the cluster emission to efficiently reject interference from laser scattering. Second, transient absorption spectra of related cluster-DNA conjugates show the dark states have broad absorption profiles that arise from electrons that are weakly bound to the nucleobases.[36] These spectra suggest that dark state absorption at 905 nm could be sufficiently strong to promote absorption. A 10% maximal enhancement of the fluorescence was observed using 9 kW/cm^2 and 110 kW/cm^2 at 690 and 905 nm, respectively (Fig. 4). As detected emission is higher energy than the secondary laser, no significant emission is observed upon 905 nm excitation alone, demonstrating that photobrightening requires both lasers. Despite the small magnitude of this effect relative to the overall signal (~10%), modulation coupled with Fourier analysis reveals the distinctive fluorescence signature of the cluster (Fig. 4). Given the short μs lifetime of the dark state, steady state populations are rapidly established, thus permitting modulation of the fluorescence on a wide range of time scales. Even using slow, 4.3 Hz square wave modulation of the 905 nm laser, the fluorescence signal is shifted away from the low frequency background that contributes to overall detection noise from unmodulated sources, thereby improving detection sensitivity. This resolution of the desired signal from the background suggests that the detection of this species in more challenging environments holds great promise.

In conclusion, DNA-encapsulated silver clusters offer the following advantages as fluorescence contrast agents: high fluorescence quantum yields, strong molar absorptivities, photostability over long time periods, persistent emission on long time scales, and relatively small sizes. Significantly, selective modulation of their emission via excited state absorption provides additional promise for discrimination in high background environments. DNA matrices stabilize clusters in aqueous environments and direct formation of specific cluster types. These studies report the formation, isolation, and identification of a near-infrared emitting, 10-Ag atom cluster that forms within $(C_3A)_2C_3TC_3A$. Its electronic transitions occur in the optimal window for biological imaging where absorption and scattering from endogenous substances is minimized. Besides this spectral advantage, this chromophore features high molecular brightness and photostability, short-time scale blinking, and

efficient light-driven depopulation of its dark state at wavelengths longer than the collected fluorescence. An important advance in characterizing cluster conjugates with DNA is the use of liquid chromatography for separation. From atomic emission studies of the near-infrared species, a relative stoichiometry of 10 Ag/oligonucleotide was derived. These studies provide the motivation to determine the stoichiometry of other silver cluster:DNA conjugates to more fully understand the factors that influence the significant variations in emission spectra that accompany changes in the DNA sequence.

Supplementary Material

Refer to Web version on PubMed Central for supplementary material.

Acknowledgments

We thank the National Science Foundation (CBET-0853692) for primary support of this work. JTP is grateful to the National Institutes of Health (R15GM071370) for primary support during the initial stages of this work. In addition, JTP thanks the National Science Foundation (CHE-0718588), Henry Dreyfus Teacher-Scholar Awards Program, and the National Institutes of Health (P20 RR-016461 from the National Center for Research Resource). RMD acknowledges NIH R01-GM086195. JTP received partial sabbatical support through matching commitments to an NSF RII Cooperative Agreement, EPS-0903795.

References

1. Frangioni JV. In vivo near-infrared fluorescence imaging. Curr Opin Chem Biol 2003;7:626–34. [PubMed: 14580568]
2. Tsien RY. Imagining imaging's future. Nat Rev Mol Celll Biol 2003;4:SS16–2221.
3. Chance B. Near-Infrared Images Using Continuous, Phase-Modulated, and Pulsed Light with Quantitation of Blood and Blood Oxygenation. Ann N Y Acad Sci 1998;838:29–45. [PubMed: 9511793]
4. Ntziachristos V, Bremer C, Weissleder R. Fluorescence imaging with near-infrared light: new technological advances that enable in vivo molecular imaging. European Radiology 2003;13:195–208. [PubMed: 12541130]
5. Pauli J, Vag T, Haag R, Spieles M, Wenzel M, Kaiser WA, Resch-Genger U, Hilger I. An in vitro characterization study of new near infrared dyes for molecular imaging. Eur J Med Chem 2009;44:3496–503. [PubMed: 19269067]
6. Waggoner A. Fluorescent labels for proteomics and genomics. Curr Opin Chem Biol 2006;10:62–6. [PubMed: 16418012]
7. Zhang J, Campbell RE, Ting AY, Tsien RY. Creating new fluorescent probes for cell biology. Nat Rev Mol Cell Biol 2002;3:906–18. [PubMed: 12461557]
8. Smith BA, Akers WJ, Leevy WM, Lampkins AJ, Xiao S, Wolter W, Suckow MA, Achilefu S, Smith BD. Optical Imaging of Mammary and Prostate Tumors in Living Animals using a Synthetic Near Infrared Zinc(II)-Dipicolylamine Probe for Anionic Cell Surfaces. J Am Chem Soc 2010;132:67–9. [PubMed: 20014845]
9. Berlier JE, Rothe A, Buller G, Bradford J, Gray DR, Filanoski BJ, Telford WG, Yue S, Liu J, Cheung CY, et al. Quantitative Comparison of Long-wavelength Alexa Fluor Dyes to Cy Dyes: Fluorescence of the Dyes and Their Bioconjugates. J Histochem Cytochem 2003;51:1699–712. [PubMed: 14623938]
10. Giepmans BN, Adams SR, Ellisman MH, Tsien RY. The fluorescent toolbox for assessing protein location and function. Science 2006;312:217–24. [PubMed: 16614209]
11. Shu X, Royant A, Lin MZ, Aguilera TA, Lev-Ram V, Steinbach PA, Tsien RY. Mammalian expression of infrared fluorescent proteins engineered from a bacterial phytochrome. Science 2009;324:804–7. [PubMed: 19423828]
12. Nienhaus GU, Wiedenmann J. Structure, Dynamics and Optical Properties of Fluorescent Proteins: Perspectives for Marker Development. Chemphyschem 2009;10:1369–79. [PubMed: 19229892]

13. Resch-Genger U, Grabolle M, Cavaliere-Jaricot S, Nitschke R, Nann T. Quantum dots versus organic dyes as fluorescent labels. Nat Methods 2008;5:763–75. [PubMed: 18756197]
14. Walling M, Novak J, Shepard JRE. Quantum Dots for Live Cell and In Vivo Imaging. International Journal of Molecular Sciences 2009;10:441–91. [PubMed: 19333416]
15. Michalet X, Pinaud FF, Bentolila LA, Tsay JM, Doose S, Li JJ, Sundaresan G, Wu AM, Gambhir SS, Weiss S. Quantum Dots for Live Cells, in Vivo Imaging, and Diagnostics. Science 2005;307:538–44. [PubMed: 15681376]
16. Allen PM, Liu W, Chauhan VP, Lee J, Ting AY, Fukumura D, Jain RK, Bawendi MG. InAs(ZnCdS) Quantum Dots Optimized for Biological Imaging in the Near-Infrared. J Am Chem Soc 2010;132:470–1. [PubMed: 20025222]
17. Kim S, Lim YT, Soltesz EG, De Grand AM, Lee J, Nakayama A, Parker JA, Mihaljevic T, Laurence RG, Dor DM, et al. Near-infrared fluorescent type II quantum dots for sentinel lymph node mapping. Nat Biotechnol 2004;22:93–7. [PubMed: 14661026]
18. Wang J, Long Y, Zhang Y, Zhong X, Zhu L. Preparation of Highly Luminescent CdTe/CdS Core/Shell Quantum Dots. Chemphyschem 2009;10:680–5. [PubMed: 19137566]
19. Petty JT, Zheng J, Hud NV, Dickson RM. DNA-templated Ag nanocluster formation. J Am Chem Soc 2004;126:5207–12. [PubMed: 15099104]
20. Richards CI, Choi S, Hsiang JC, Antoku Y, Vosch T, Bongiorno A, Tzeng YL, Dickson RM. Oligonucleotide-Stabilized Ag Nanocluster Fluorophores. J Am Chem Soc 2008;130:5038–9. [PubMed: 18345630]
21. Gwinn EG, O'Neill P, Guerrero AJ, Bouwmeester D, Fygenson DK. Sequence-Dependent Fluorescence of DNA-Hosted Silver Nanoclusters. Adv Mater 2008;20:279–83.
22. Sharma J, Yeh HC, Yoo H, Werner JH, Martinez JS. A complementary palette of fluorescent silver nanoclusters. Chem Commun 2010;46:3280–2.
23. Vosch T, Antoku Y, Hsiang JC, Richards CI, Gonzalez JI, Dickson RM. Strongly emissive individual DNA-encapsulated Ag nanoclusters as single-molecule fluorophores. Proc Natl Acad Sci U S A 2007;104:12616–21. [PubMed: 17519337]
24. Richards CI, Hsiang JC, Senapati D, Patel S, Yu J, Vosch T, Dickson RM. Optically Modulated Fluorophores for Selective Fluorescence Signal Recovery. J Am Chem Soc 2009;131:4619–21. [PubMed: 19284790]
25. Sengupta B, Springer K, Buckman JG, Story SP, Abe OH, Hasan ZW, Prudowsky ZD, Rudisill SE, Degtyareva NN, Petty JT. DNA Templates for Fluorescent Silver Clusters and I-Motif Folding. J Phys Chem C 2009;113:19518–24.
26. O'Neill PR, Velazquez LR, Dunn DG, Gwinn EG, Fygenson DK. Hairpins with Poly-C Loops Stabilize Four Types of Fluorescent Agn:DNA. J Phys Chem C 2009;113:4229–33.
27. Huber CG, Oberacher H. Analysis of nucleic acids by on-line liquid chromatography-Mass spectrometry. Mass Spectrom Rev 2001;20:310–43. [PubMed: 11948655]
28. Bonacic-Koutecky V, Veyret V, Mitric R. Ab initio study of the absorption spectra of Ag-n (n=5–8) clusters. J Chem Phys 2001;115:10450–60.
29. Zheng J, Nicovich PR, Dickson RM. Highly Fluorescent Noble-Metal Quantum Dots. Annu Rev Phys Chem 2007;58:409. [PubMed: 17105412]
30. Umezawa K, Matsui A, Nakamura Y, Citterio D, Suzuki K. Bright, Color-Tunable Fluorescent Dyes in the Vis/NIR Region: Establishment of New ldquoTailor-Maderdquo Multicolor Fluorophores Based on Borondipyrromethene. Chem Eur J 2009;15:1096–106.
31. Krichevsky O, Bonnet G. Fluorescence correlation spectroscopy: the technique and its applications. Rep Prog Phys 2002;65:251–97.
32. Lavis LD, Raines RT. Bright Ideas for Chemical Biology. ACS Chem Biol 2008;3:142–55. [PubMed: 18355003]
33. Yip WT, Hu D, Yu J, Vanden Bout DA, Barbara PF. Classifying the Photophysical Dynamics of Single- and Multiple-Chromophoric Molecules by Single Molecule Spectroscopy. J Phys Chem A 1998;102:7564–75.
34. Widengren J, Seidel CAM. Manipulation and characterization of photo-induced transient states of Merocyanine 540 by fluorescence correlation spectroscopy. PCCP 2000;2:3435–41.

35. Ringemann C, Schönle A, Giske A, von Middendorff C, Hell SW, Eggeling C. Enhancing Fluorescence Brightness: Effect of Reverse Intersystem Crossing Studied by Fluorescence Fluctuation Spectroscopy. ChemPhysChem 2008;9:612–24. [PubMed: 18324718]

36. Patel SA, Cozzuol M, Hales JM, Richards CI, Sartin M, Hsiang JC, Vosch T, Perry JW, Dickson RM. Electron Transfer-Induced Blinking in Ag Nanodot Fluorescence. J Phys Chem C 2009;113:20264–70.

37. Richards CI, Hsiang JC, Dickson RM. Synchronously Amplified Fluorescence Image Recovery (SAFIRe). J Phys Chem B 2010;114:660–5. [PubMed: 19902923]

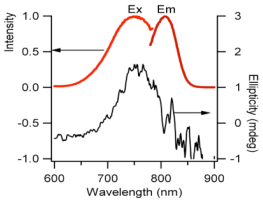

Figure 1.

Fluorescence excitation and emission (left axis) and circular dichroism (right axis) spectra of the near infrared emissive silver cluster that forms with $(C_3A)_2C_3TC_3A$. The abscissas for the fluorescence spectra are relative intensities.

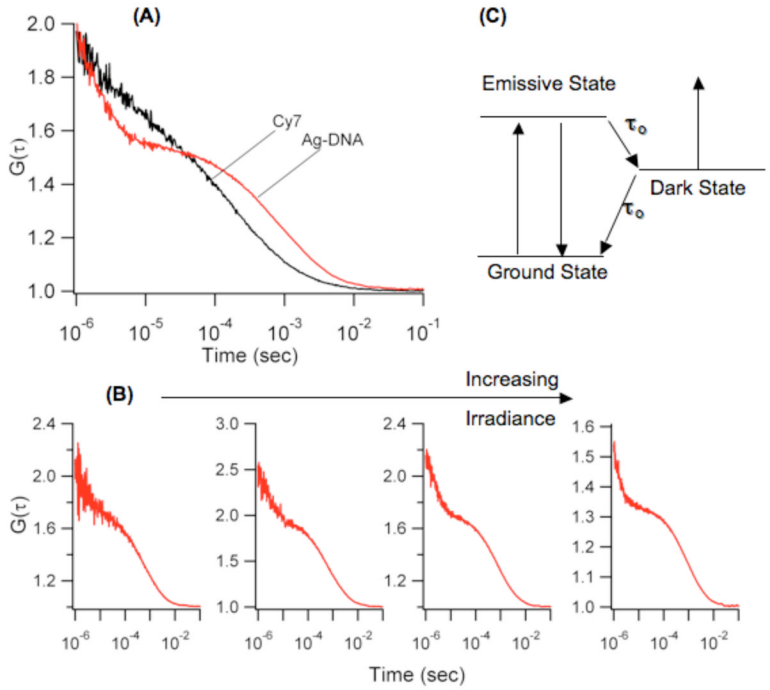

Figure 2.

(A) Fluorescence autocorrelation functions for Cy7 (black) and the silver-DNA conjugate (red) emphasize the longer diffusion time of the latter through the laser probe volume. (B) Dependence of the shorter time scale dynamics on laser irradiance at 730 nm. Proceeding from the left, the irradiances are 0.3, 2, 5, and 30 kW/cm^2. (C) Schematic energy level diagram rationalizing the photophysical behavior of the cluster-DNA conjugates. Fluorescence is derived from cycling through the ground and emissive states. Transitions into and from the dark state are determined by τ_{on} and τ_{off}, respectively. Decay from this state is occurs by both natural decay and optical excitation.

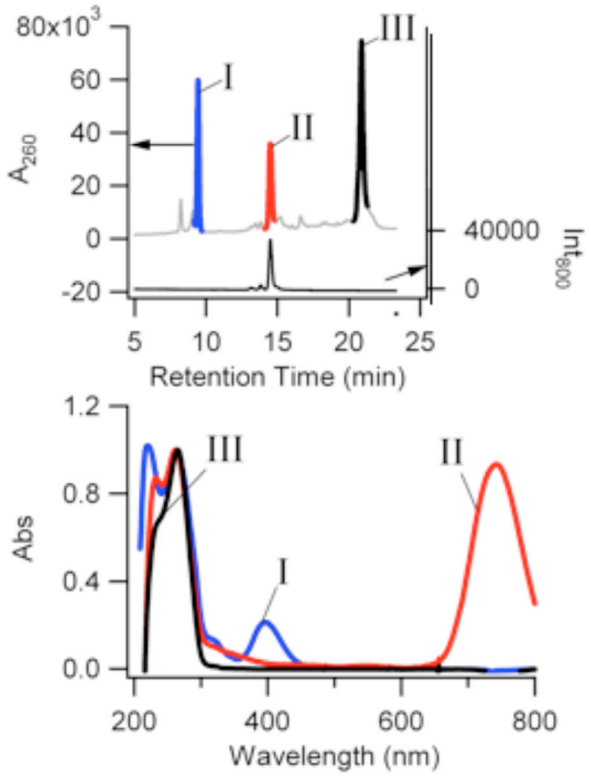

Figure 3.
(Top) Chromatograms derived using the absorbance at 260 nm (left axis) and 800nm fluorescence (right axis) for the cluster-DNA conjugates. (Bottom) Spectra for the fractions associated with Peaks I, II, and III from the above chromatogram.

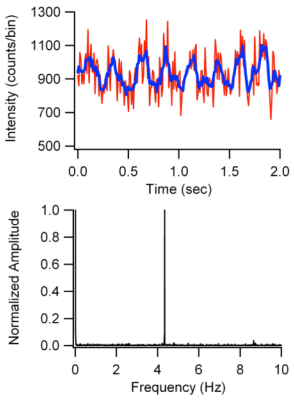

Figure 4.

(Top) Fluorescence intensity (counts/0.01 s bins) of the cluster when illuminated by a 690 nm laser and a 4.3 Hz modulated 905 nm laser. Smoothed data (blue trace) help demonstrate the periodic intensity changes. (Bottom) Fourier analysis of modulated fluorescence intensity data.

Table 1

Comparison of τ_{on} and τ_{off} for the dark state associated with the near-infrared emitting silver cluster under 730nm cw excitation (no secondary laser).

τ_{on} (μs)	τ_{off} (μs)	Irradiance (kW/cm^2)
14	7	1.6
8	6	2.2
6	5	4.8
5	4.5	8
5	4	14
5	3	66